J|A|C|S
ARTICLES

Published on Web 08/01/2008

High Carrier Density and Capacitance in TiO_2 Nanotube Arrays Induced by Electrochemical Doping

Francisco Fabregat-Santiago,*,† Eva M. Barea,† Juan Bisquert,*,† Gopal K. Mor,‡ Karthik Shankar,‡ and Craig A. Grimes*,‡

Departament de Física, Universitat Jaume I, 12071 Castelló de la Plana, Spain, and Department of Electrical Engineering, Materials Research Institute, The Pennsylvania State University, University Park, Pennsylvania 16802

Received December 6, 2007; E-mail: fabresan@fca.uji.es; bisquert@fca.uji.es; cgrimes@engr.psu.edu

Abstract: The paper describes the electronic charging and conducting properties of vertically oriented TiO_2 nanotube arrays formed by anodization of Ti foil samples. The resulting films, composed of vertically oriented nanotubes approximately 10 μm long, wall thickness 22 nm, and pore diameter 56 nm, are analyzed using impedance spectroscopy and cyclic voltammetry. Depending on the electrochemical conditions two rather different electronic behaviors are observed. Nanotube array samples in basic medium show behavior analogous to that of nanoparticulate TiO_2 films used in dye-sensitized solar cells: a chemical capacitance and electronic conductivity that increase exponentially with bias potential indicating a displacement of the Fermi level. Nanotube array samples in acidic medium, or samples in a basic medium submitted to a strong negative bias, exhibit a large increase in capacitance and conductivity indicating Fermi level pinning. The contrasting behaviors are ascribed to proton intercalation of the TiO_2. Our results suggest a route for controlling the electronic properties of the ordered metal-oxide nanostructures for their use in applications including supercapacitors, dye-sensitized solar cells, and gas sensing.

1. Introduction

Dye-sensitized solar cells (DSCs) are being increasingly investigated as a viable photovoltaic technology. The standard DSC configuration uses a porous TiO_2 film consisting of a disordered network of colloidal nanoparticles about 10 nm in diameter[1] deposited on a conducting substrate, then sintered at $\approx$500 °C to ensure good electrical connectivity between the nanoparticles. Although such DSCs have been able to achieve photoconversion efficiencies of 11%[2] DSCs composed of ordered nanoarchitectures such as nanowires and nanotubes, vertically oriented from the substrate, have raised considerable interest. The ordered material architecture offers the benefits of (i) more direct transport pathways uninterrupted by interparticle connections, (ii) the possibility to form surface electrical fields that should reduce recombination by confining the injected electrons in the central zone of the tubes,[3] and (iii) superior void penetration of the organic hole conductor in preparation of solid-state DSCs due to the less intricate shape of the nanostructure.[4]

Several metal-oxide nanowire and nanotube architectures deposited on a conducting substrate for DSC application have recently been reported, with the majority of studies focusing on use of TiO_2[5–8] and ZnO.[3,9–11] A crucial property determining the photovoltaic performance of these semiconducting nanostructured films is the electronic carrier density, which is in turn dependent on the dopant level; carrier density plays a key role in determining electronic conductivity.

The carrier density and dopant level in nanostructured films may vary widely depending on the materials, method of preparation, architecture, and electrochemical or thermal treatments. One can generally distinguish two basic limiting situations.[12] First, standard colloidal TiO_2 films for DSCs made of small, $\approx$10 nm diameter, nanoparticles usually show very low (unmeasurable) charge carrier densities since the dopant levels are minimal and the equilibrium Fermi level is far from the conduction band. When the Fermi level is raised by a bias potential the films respond with a chemical capacitance that normally displays an exponential bias dependence reflecting the density of localized states (DOS) in the band gap.[13] Over

† Universitat Jaume I.
‡ The Pennsylvania State University.

(1) O'Regan, B.; Grätzel, M. *Nature* **1991**, *353*, 737.
(2) Wang, Q.; Ito, S.; Grätzel, M.; Fabregat-Santiago, F.; Mora-Seró, I.; Bisquert, J.; Bosshoa, T.; Imaic, H. *J. Phys. Chem. B* **2006**, *110*, 19406.
(3) Mora-Seró, I.; Fabregat-Santiago, F.; Denier, B.; Bisquert, J.; Tena-Zaera, R.; Elias, J.; Lévy-Clement, C. *Appl. Phys. Lett.* **2006**, *89*, 203117.
(4) Snaith, H. J.; Schmidt-Mende, L. *Adv. Mater.* **2007**, *19*, 3187.
(5) Mor, G. K.; Shankar, K.; Paulose, M.; Varghese, O. K.; Grimes, C. A. *Nano Lett.* **2006**, *6*, 215.
(6) Mor, G. K.; Varghese, O. K.; Paulose, M.; Shankar, K.; Grimes, C. A. *Sol. Energy Mater. Sol. Cells* **2006**, *90*, 2011.
(7) Shankar, K.; Mor, G. K.; Prakasam, H. E.; Yoriya, S.; Paulose, M.; Varghese, O. K.; Grimes, C. A. *Nanotechnology* **2007**, *18*, 065707.
(8) Enache-Pommer, E.; Boercker, J. E.; Aydil, E. S. *Appl. Phys. Lett.* **2007**, *91*, 123116.
(9) Baxter, J. B.; Aydil, E. S. *Appl. Phys. Lett.* **2005**, *86*, 053114.
(10) Martinson, A. B. F.; McGarrah, J. E.; Parpia, M. O. K.; Hupp, J. T. *Phys. Chem. Chem. Phys.* **2006**, *8*, 4655–4659.
(11) Martinson, A. B. F.; Elam, J. W.; Hupp, J. T.; Pellin, M. J. *Nano Lett.* **2007**, *7*, 2183.
(12) Bisquert, J. *Phys. Chem. Chem. Phys.* **2008**, *10*, 49.
(13) Bisquert, J.; Fabregat-Santiago, F.; Mora-Seró, I.; Garcia-Belmonte, G.; Barea, E. M.; Palomares, E. *Inorg. Chim. Acta* **2008**, *361*, 684–698.

 10.1021/ja710899q CCC: $40.75

prolonged operation the DOS can be modified by cation intercalation in the TiO_2 nanoparticle bulk.[14]

Relevant to our forthcoming discussion, we note as-synthesized films composed of ZnO nanowires[3] several micrometers long with relatively large diameters (about 100 nm) display a large degree of doping (about 10^{19} cm^{-3}). Therefore, these nanowires can sustain internal band bending at the surface and are characterized by a depletion layer at the semiconductor/electrolyte interface with a highly conducting central region, providing a dielectric capacitance when tested electrochemically.[3]

Potentiostatic anodization constitutes a versatile method to prepare vertically oriented TiO_2 nanotube array films which have shown excellent performance in a variety of applications including photovoltaics, the solar generation of hydrogen by water photoelectrolysis, and gas sensing.[5–7] In these nanotube array films, the wall thickness is of the order of 20 nm (controllable from ≈5 to 35 nm), while the length can be easily varied from 200 nm to 1000 μm.[7–9] Therefore, the geometry can be viewed as a combination of the characteristic DSC nanoparticle size in the radial direction, with a macroscopic continuous pathway in the axial direction. The characteristic carrier density and electrical field distribution is not a priori clear, i.e., whether the film should respond with a chemical capacitance, or with some other behavior, and this is investigated in the present paper. We use impedance spectroscopy to analyze a range of nanotube array samples of different lengths. The simultaneous detection of transport resistance and capacitance informs us of the carrier density dependence on the potential.

2. Experimental Section

TiO_2 nanotube arrays films were made by anodic oxidation of titanium foil (250 μm thick, 99.8% purity, Sigma-Aldrich) at a constant voltage of 20 V in 0.27 M tetrabutylammonium fluoride solution prepared in formamide containing 3.0% deionized water.[5] As-anodized samples were first thoroughly rinsed with ethanol, then with water, followed by ultrasonication cleaning in ethanol for a few seconds. Finally, the samples were dried under nitrogen. Sample morphology was determined using field emission scanning electron microscopy (FESEM). The ultrasonically cleaned samples have no debris, i.e., solution precipitate, on top of the tubes. The outer diameter, inner diameter, and the wall thickness of the nanotubes are, respectively, 100, 56, and 22 nm. Anodization time was varied from 30 min to 12 h to obtain tube lengths from 1.5 to 20 μm. A typical top and cross-sectional view of an approximately 8 μm long TiO_2 nanotube array film is shown in Figure 1. All samples were crystallized by annealing in oxygen gas at 525 °C for 2 h with a ramp-up and ramp-down rate of 1 °C/min; the crystallized nanotubes are anatase with a thermally grown rutile layer underneath.[4]

DSCs were prepared in the following manner: After being immersed in dye solution (N719 0.3 mM in ethanol) overnight the nanotube array electrode was clamped between two glass sheets, one of them thermally platinized TCO glass (Pilkington TEC15, 15 Ω/sq sheet resistance) with 30 μm suryline tape spacer. The cell was then filled with a drop of electrolyte (0.5 M LiI, 0.05 M I_2, and 0.5 M MBI in acetonitrile). The nanotubes were illuminated at 30 mW cm^{-2} with a 1.5 a.m. filtered Xe lamp (Oriel).

Voltammetric and impedance spectroscopy measurements were performed using TiO_2 nanotube samples of variable length: 1.5, 5, 8, 10, and 20 μm. Voltammetric and impedance spectroscopy measurements were performed with an Autolab PGSTAT-30 potentiometer in two potential ranges: between 0.1 and −0.75 V for both acidic and basic media, aqueous solutions adjusted to pH 11 with KOH and pH 2 with H_2SO_4, and from 0.1 V up to −1.5 V for basic media. Potentials are reported versus a Ag/AgCl (3 M KCl) reference electrode; hence, there is a −0.31 V offset between DSC and electrochemical potentials (I_3^-/I^- redox potential vs Ag/AgCl reference electrode).

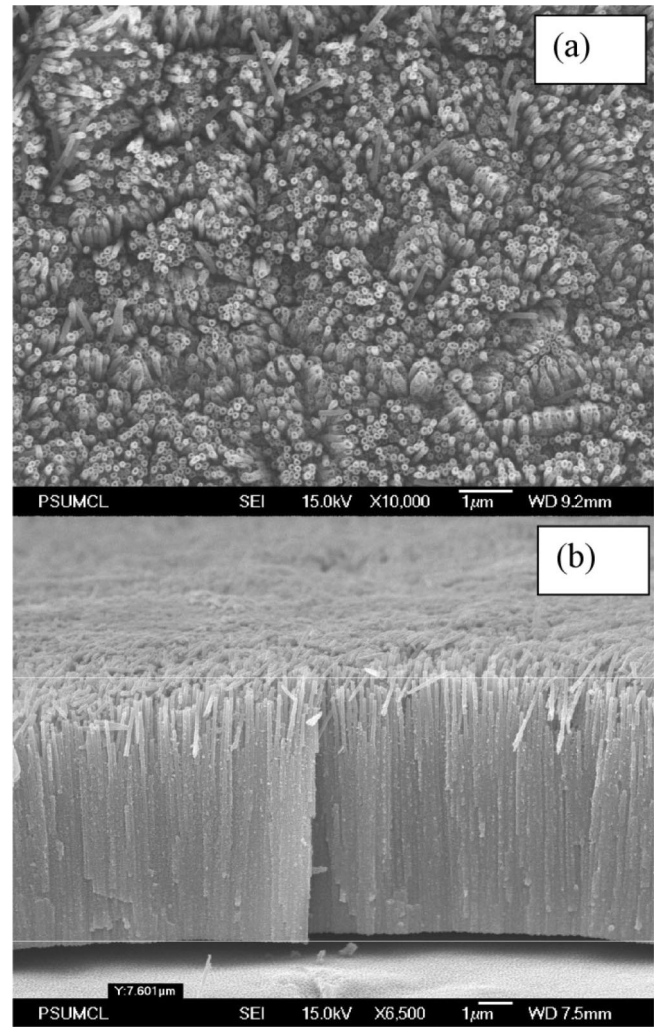

Figure 1. FESEM views of the TiO_2 nanotubes (length ~8 μm): (a) top view, (b) cross section.

3. Model

For an array of TiO_2 column-like tubes of length (height) L immersed in an electrolyte, we expect to find the typical impedance behavior of the porous electrode described by a transmission line model shown in Figure 2a:[15,16]

$$Z(\omega) = \left(\frac{R_{tr}R_{ct}}{1 + i\omega/\omega_{rec}}\right)^{1/2} \coth[(R_t/R_{ct})^{1/2}(1 + i\omega/\omega_{rec})^{1/2}] \quad (1)$$

Here R_{tr} is the total transport resistance, R_{ct} is the charge-transfer resistance at the solid/electrolyte interface along the resistive transport channel. ω_{rec} is the radian frequency of the charge-transfer process, $\omega_{rec} = (R_{ct}C_3)^{-1}$, related to electron

(14) Kopidakis, N.; Benkstein, K. D.; van de Lagemaat, J.; Frank, A. J. *J. Phys. Chem. B* **2003**, *107*, 11307.
(15) Bisquert, J.; Garcia-Belmonte, G.; Fabregat-Santiago, F.; Ferriols, N. S.; Bogdanoff, P.; Pereira, E. C. *J. Phys. Chem. B* **2000**, *104*, 2287.
(16) Bisquert, J. *J. Phys. Chem. B* **2002**, *106*, 325.

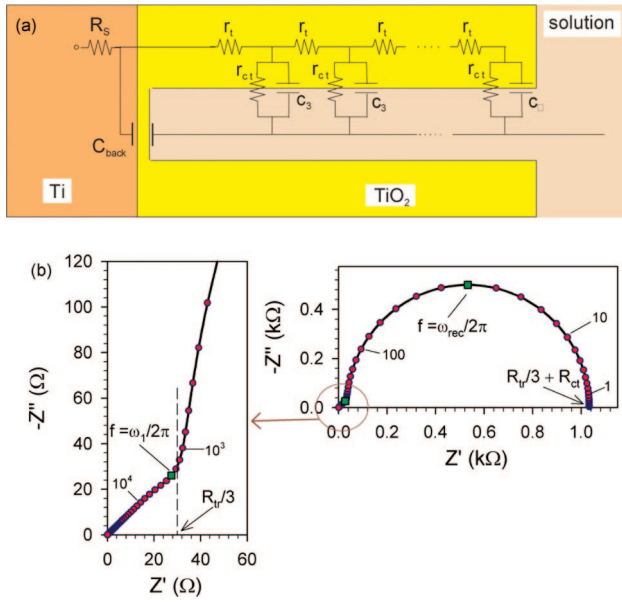

Figure 2. (a) Transmission line equivalent circuit model applied to the TiO_2 nanotube array films. (b) Characteristic impedance response of a nanotube electrode. The large arc is the parallel combination of R_{ct} and C_3. The left panel shows in expansion the high-frequency 45°-like behavior due to transport of electrons in the semiconductor. The frequencies ω_1 and ω_{rec} are defined in the main text.

lifetime[17] by $\tau_n = \omega_{rec}^{-1}$. C_3 is the total capacitance in the solid phase and the solid−electrolyte interface. C_3 has several possible contributions:[18] (1) the chemical capacitance of the semiconductor, C_μ, (2) the depletion capacitance in the semiconductor surface, C_{dpl}, and (3) the Helmholtz capacitance of the surface, C_H. Total film capacitance has an additional contribution from the exposed surface of the barrier layer at the bottom of the columns, C_{back}, see Figure 2a.

In the case of low reactivity with respect to electron transport, as given by the condition $R_{ct} > R_t$,[15] for frequencies higher than $\omega_1 = (R_t C_3)^{-1}$ eq 1 reduces to

$$Z = \left(\frac{R_{tr}}{C_3}\right)^{1/2} (i\omega)^{-1/2} \qquad (2)$$

Equation 2 is often termed the "Warburg" impedance, appearing as a 1-slope line in the complex impedance plot shown in the left of Figure 2b. It should be emphasized that, in contrast to semi-infinite diffusion, in the transmission line model the 45° characteristic appears only in the high-frequency part of the impedance spectrum. As the frequency decreases ($\omega < \omega_1$) the charge-transfer resistance gives rise to a semicircle at low frequency, consisting of the parallel combination of R_{ct} and C_3 as shown in the right of Figure 2b.

The nanotube array presents the characteristic behavior of nanoparticulate TiO_2 networks usually found in DSCs[2,19,20] with little *intrinsic* doping by foreign atoms and consequently a homogeneous conduction band level throughout the semiconductor. The bias potential V determines the Fermi level position

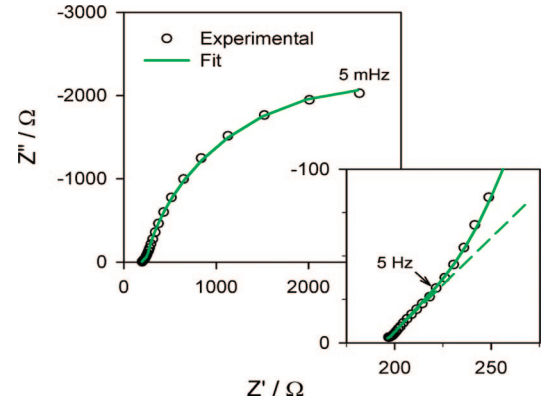

Figure 3. Impedance spectra of a TiO_2 nanotube array film initially held at −1 V for 20 min, i.e., "aged", pH 11, showing typical transmission line behavior with low-frequency recombination arc and high-frequency 45° line. Impedance was performed at −0.7 V.

with respect to the conduction band, whereas the transport resistance in the TiO_2 displays the potential dependence[2]

$$R_{tr} = R_{0tr} \exp\left[\frac{qV}{kT}\right] \qquad (3)$$

with q the elementary positive charge. R_{tr} is large at low potentials due to the absence of free carriers; therefore, no contribution from the TiO_2 nanotubes to capacitance and charge-transfer resistance is expected. In this regime the majority of the cell capacitance will come from the exposed barrier layer, with a value of the order of 10 $\mu F \cdot cm^{-2}$. The TiO_2 capacitance increases with applied potential by[21]

$$C_\mu = C_{0\mu} \exp\left[-\alpha\frac{qV}{kT}\right] \qquad (4)$$

with $\alpha < 1$, until it reaches the value of the C_H given by the total surface of the tubes.

4. Results and Discussion

Electrochemical measurement of the nanotube array samples provided a variety of behaviors that we analyze on a case by case basis. First, while keeping the samples in a basic (pH 11) electrolyte medium at moderate applied potentials (<1 V), they presented the general behavior described by eq 1, shown in Figure 3. The parameter values obtained from impedance (C_3, R_{tr}, R_{ct}) follow quite accurately the trends stated in eqs 3 and 4. The resulting parameters for the 10 μm sample are shown in Figure 4, with a chemical capacitance value of $\alpha = 0.21$, charge-transfer resistance coefficient of 0.40, and transport resistance slope of 84 mV/decade, the values of which are comparable to those obtained for nanocolloid-based films.[2,13,19,20] The clear experimental observation of transmission line behavior (Figure 3) indicates that the capacitance and charge-transport resistance are due to the electronic response of the TiO_2 nanotubes, whereas the impedance behavior can be unambiguously interpreted in terms of the model of Figure 2a providing information on the carrier distribution within the tubes. As seen in Figure 4 when the applied bias potential was brought to large negative values (< −1.5 V) or kept at moderate potentials (≈ −1 V for more than 20 min) in basic media, the impedance results changed dramatically. The transport resistance is reduced and maintains a nearly constant value, indicating a large charge carrier density insensitive to applied voltage. This is a strong indication of highly doped behavior. In addition, the chemical

(17) Bisquert, J.; Zaban, A.; Greenshtein, M.; Mora-Seró, I. *J. Am. Chem. Soc.* **2004**, *126*, 13550.
(18) Bisquert, J. *Phys. Chem. Chem. Phys.* **2003**, *5*, 5360.
(19) Fabregat-Santiago, F.; Bisquert, J.; Garcia-Belmonte, G.; Boschloo, G.; Hagfeldt, A. *Sol. Energy Mater. Sol. Cells* **2005**, *87*, 117.
(20) Bisquert, J. *Phys. Chem. Chem. Phys.* **2008**, *10*, 3175.

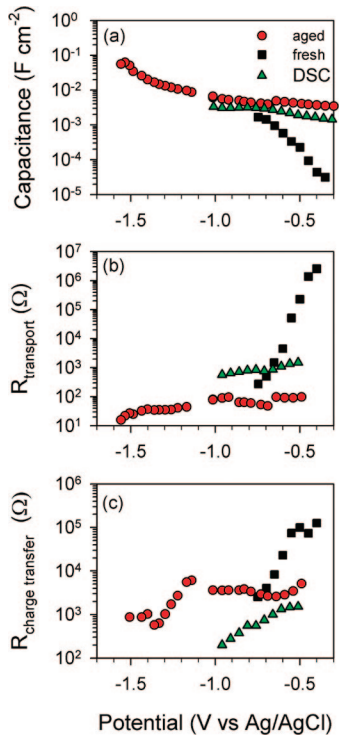

Figure 4. Comparison of parameters from impedance data, from the equivalent circuit model of Figure 2a, as a function of electrode potential, for a 10 μm sample before (fresh) and after being held at −1 V for 20 min in basic solution (aged), and in a DSC. (a) Capacitance per unit geometric area, C_3, (b) transport resistance, and (c) charge-transfer resistance. Note that for comparison DSC values have been shifted −0.31 V (I_3^-/I^- redox potential vs Ag/AgCl reference electrode).

capacity of TiO_2 increases enormously, with values ranging from 1 to 6 mF·cm^{-2} at low potentials, reaching close to 80 mF·cm^{-2} at the highest applied potential. These values approach those of supercapacitors (≈0.3−1 F·cm^{-2}),[21] see Figure 4a. Larger values of capacitance are obtained with increasing nanotube length. We attribute the observed modifications under large negative bias in basic medium to proton uptake in the nanotube walls, which also changed the clear walls to a blue color. Proton uptake in nanocrystalline TiO_2 was demonstrated by Hupp and co-workers using a photoelectrochemical quartz crystal microbalance technique.[22,23] Proton intercalation within the TiO_2 nanotubes results in free electrons that, in turn, decrease the electrical resistance. The cation intercalation results in a much larger capacitance, most likely due to formation of a depletion region at the semiconductor surface.[24] Figure 5a shows cyclic voltammetric measurements of a 10 μm long nanotube sample prior to and after proton intercalation. The capacitive current[25] is much higher for the cation-intercalated films indicating a great increase in the capacitance at low potentials. Figure 5b shows the dynamic intercalation process in an 8 μm sample.

During the first cathodic scan, starting at 0 V, at low negative potentials the capacity is small, whereas in the return anodic scan the capacitance is much larger. In the second cathodic scan the capacitance is large even at low potentials and, with respect to the first scan, further increases in the anodic return.

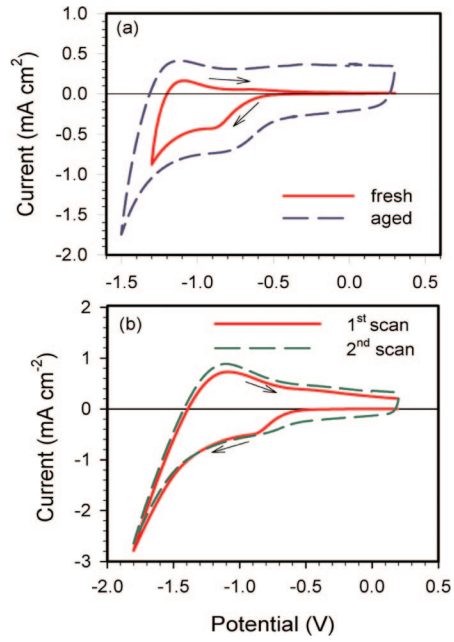

Figure 5. (a) Cyclic voltammetries of a 10 μm sample before (fresh) and after application of a strong bias potential (aged) while measuring impedance. (b) The intercalation process during a voltammetry of sufficient potential in a 8 μm long nanotube array sample.

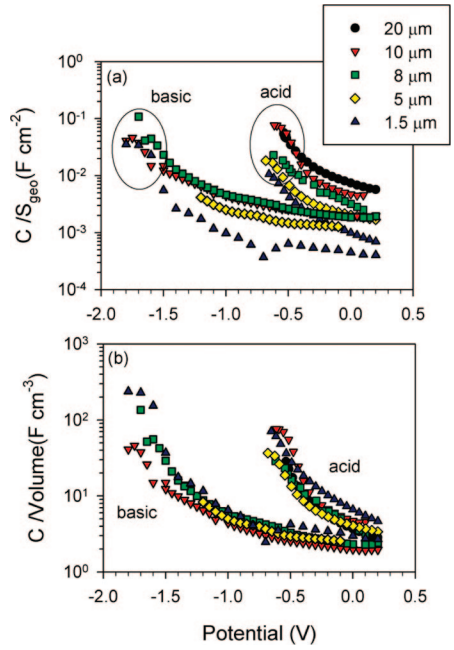

Figure 6. (a) Capacitance of TiO_2 nanotubes, per unit geometric area of the film, in basic and acidic media. (b) Same capacitance data rescaled to volume density, by dividing by nanotube length.

Measurements were also done in acidic media (pH 2), and in this case high capacitance values were observed in all samples, see Figure 6a. The transport resistance is so low it cannot be reliably measured. The capacitance increase at the highest negative potentials appears due to the unpinning of the Fermi level that occurs at potentials more negative than −0.8 V allowing the Fermi level to approach the conduction band.[25] The results indicate that the nanotube array samples are proton-

(21) Winter, M.; Brodd, R. J. *Chem. Rev.* **2004**, *104*, 4245.
(22) Lemon, B. I.; Hupp, J. T. *J. Phys. Chem.* **1996**, *100*, 14578.
(23) Yan, S. G.; Hupp, J. T. *J. Phys. Chem.* **1996**, *100*, 2667.
(24) Muñoz, A. G. *Electrochim. Acta* **2007**, *52*, 4167.
(25) Fabregat-Santiago, F.; Mora-Seró, I.; Garcia-Belmonte, G.; Bisquert, J. *J. Phys. Chem. B* **2003**, *107*, 758.
(26) Fabregat-Santiago, F.; Bisquert, J.; Palomares, E.; Otero, L.; Kuang, D.; Zakeeruddin, S. M.; Gratzel, M. *J. Phys. Chem. C* **2007**, *111*, 6550.

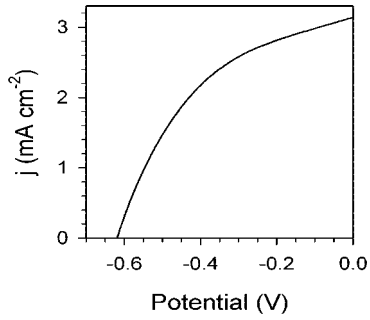

Figure 7. Current density−potential curve of a DSC made from a 10 μm nanotube film "aged" by being held at −1 V for 20 min.

intercalated even in the absence of the negative bias that was required in basic media.

Figure 6 enables comparison of the capacitance behavior of the nanotube array films as a function of nanotube array length in both basic and acid electrolytes. We note the displacement of the capacitance values along the voltage axis, which is expected by the change of the TiO_2 conduction band at different pH values. The capacitance scales with nanotube length. The small dispersion of the rescaled values in Figure 6b is attributed to minor differences in wall thickness of the different samples. In summary, it is observed that "fresh" nanotube array samples in basic medium display the standard behavior of crystalline TiO_2 nanoparticles, consisting of initially low conductivity and chemical capacitance that exponentially increase with bias potential.[2,19] These properties change dramatically upon negative bias, whereupon the sample displays the behavior characteristic of a highly doped semiconductor, i.e., a high capacitance and a low charge-transport resistance nearly independent of bias. We attribute this change to the intercalation of protons from water into the nanotubes. In acidic media the high proton concentration of the electrolyte facilitates intercalation, whereas in basic solution it requires application of a negative potential. Further quantitative analysis of the capacitance data to extract the volume density of carriers requires an extension of the Mott−Schottky model in cylindrical coordinates[3] to match the tubular geometry and consideration of the frequency effect of band gap states.[24]

4.1. Dye Solar Cell Characterization. Back-side-illuminated DSCs were fabricated using a 10 μm long TiO_2 nanotube array film on a Ti foil substrate. Prior to DSC fabrication the nanotube array film was held at −1 V for 20 min in acidic solution. Considering our previous discussion, the performance of the electron-transporting nanotube arrays are expected to be altered by proton intercalation. From the current density−potential ($j-V$) curve, Figure 7, we obtain an efficiency of 3.1%, short-circuit current of 3.1 mA cm^{-2}, photopotential 0.63, and fill factor of 0.44. Although unoptimized, this DSC is significantly less efficient than previous reports for the same device geometry.[5–7] The impedance measurements of Figure 4 allow us to identify the central factors determining the relatively poor shape of the $j-V$ curve:[26,27]

(i) The high capacitance obtained for the DSC, Figure 4a, indicates that the TiO_2 nanotubes have been cation-intercalated. This property may limit the movement of the Fermi level in the semiconductor, thus limiting V_{oc}.

(ii) The recombination resistance, Figure 4c, is comparatively low[19,26] indicating that cation intercalation, or doping, enhances recombination. It appears enhanced recombination is responsible for the pronounced slope at low potentials in the DSC which contributes to a reduction in the fill factor and, additionally, limits V_{oc}.[26,27]

(iii) TiO_2 intercalation, observed through capacitance measurements, is confirmed by the nearly constant value obtained for the transport resistance. The values obtained for R_{tr} in the DSC samples are higher than expected. These transport resistance values accurately describe the slope of the $j-V$ curve at high negative potentials, related to a high overall series resistance and poor fill factor.[26,27] The contributions to the overall resistance found for these DSC samples were 20 Ω from the conducting glass and titanium foil, 7 Ω from the Pt counter electrode, from 20 to 100 Ω (depending on the potential) from the diffusion of the redox in the electrolyte, and values above 200 Ω ($= R_{tr}/3$[16]) from electron transport in the TiO_2.

From these results we can infer that *unintentional* doping, i.e., intercalation, may have detrimental effects on DSC performance due mainly to the pinning of the Fermi level and increase of recombination. Strategies for improving DSC performance by electrochemical doping include the formation of fast transport states[28] and the formation of core−shell or graded doping of the metal-oxide including a fast transport channel.[29] Such approaches could decrease the electron-transport resistance to improve the photocurrent while allowing for Fermi level displacement and consequently a larger photovoltage. The possibility of unwanted TiO_2 intercalation suggests long-term DSC stability may be enhanced by substitution of the lithium ions by larger ones such as tetrabutylammonium or guanidinium.

5. Conclusions

The carrier density in TiO_2 nanotube array films may present very different behaviors depending on the electrolyte and electrochemical treatment. In basic media the films display the standard behavior of nanoparticulate TiO_2 films with a chemical capacitance exponentially dependent on the bias potential. This can be modified to demonstrate a very high capacitance, due we believe to the intercalation of protons into the TiO_2, offering the possibility for application in supercapacitors. Proton intercalation, or doping of the nanotubes in acidic media, is readily achieved, whereas that in basic media requires application of strong negative potentials. DSCs prepared with the nanotubes previously intercalated with protons from solution showed limited performance. In this case charge transport within the titanium dioxide was found to be the main contribution to the DSC series resistance. Our results show that impedance spectroscopy is an effective tool for in situ investigation of the conduction and accumulation properties of advanced metal-oxide architectures for enhanced DSC operation.

Acknowledgment. J.B. acknowledges financial support from Ministerio de Educacion y Ciencia under projects MAT2007-62982 and HOPE CSD2007-00007 (Consolider-Ingenio 2010). C.A.G. acknowledges financial support from the Department of Energy DE-FG02-06ER15772.

JA710899Q

(27) Sze, S. M. *Physics of Semiconductor Devices*, 2nd ed.; John Wiley and Sons: New York, 1981.

(28) Wang, Q.; Zhang, Z.; Zakeeruddin, S. M.; Gratzel, M. *J. Phys. Chem. C* **2008**, *112*, 7084.

(29) Chappel, S.; Grinis, L.; Ofir, A.; Zaban, A. *J. Phys. Chem. B* **2005**, *109*, 1643.